Soils and Rocks
An International Journal of Geotechnical and Geoenvironmental Engineering
www.soilsandrocks.com
ISSN 1980-9743
ISSN-e 2675-5475

Radial consolidation considering Newtonian and non-Newtonian viscous components of the effective stress

Raphael Felipe Carneiro[1#], Ian Schumann Marques Martins[2], Denise Maria Soares Gerscovich[3]

Article

Keywords
Secondary compression
Radial flow
Viscosity
Strain rate

Abstract

Research on the viscous behavior of soft soils suggested that the effective stress should be divided into two components. One is related to the solid contacts between the grains, and its variation would be the true cause of deformations and distortions. The other is related to the viscous contacts of the water adsorbed to the grains, which would not cause deformations or distortions, and would be a function of the strain rate. This model is able to explain some phenomena, such as secondary consolidation and the increase in pore pressure after drainage closure. However, a consolidation theory adopting a linear relationship between the viscous component and the strain rate (Newtonian behavior) could not reproduce the secondary consolidation as seen in consolidation tests. In this paper, three theories of radial flow consolidation were developed and solved analytically. In two of them the linear relationship was adopted, while in the third one a non-linear relationship was proposed (non-Newtonian behavior). The solutions showed that the linear relationship is in fact not able to reproduce secondary consolidation, but the non-linear relationship provided much better results and can be a promising tool for future studies.

1. Introduction

Terzaghi (1941) suggested the intergranular contacts in a soft soil could be divided into two types of contacts. These are the solid contacts, which occur in the vicinity of the surface of the particles, and viscous contacts, which occur in the water adsorbed to the grains. Both contacts transmit intergranular force, thus it would be necessary to subdivide the effective stresses into two components as well.

Terzaghi (1941) used this concept to explain secondary compression. During consolidation, after almost all the excess pore pressure has dissipated ("end" of primary consolidation), relative motion between particles continues until all viscous contacts become solid contacts. This gradual movement of the particles over time is then called secondary consolidation.

Taylor (1942) proposed that clays have an additional resistance, called "plastic structural resistance", which is a non-linear function of the strain rate. It is subdivided into two parts: "viscous structural resistance", which acts during primary consolidation, and "bond resistance", which acts during secondary consolidation. Taylor (1942) simplified the plastic structural resistance to a linear function of the strain rate in order to develop a consolidation theory, but it was restricted to primary consolidation.

Leroueil et al. (1985) performed constant rate of strain (CRS) tests on clay specimens from Canada, with different strain rates. The results showed that the lower the strain rate, the more the compression curve shifts to the left. There would therefore be a limiting compression curve on the left, representing a zero strain rate.

Martins (1992) argued that some phenomena, such as stress relaxation and the increase in pore pressure after drainage closure, contradict Terzaghi's Principle of Effective Stress (see Atkinson & Bransby, 1978). Martins (1992) then suggested that the influence of the strain rate is the missing piece for the completeness of the Principle of Effective Stress, and proposed that the shear strength of soft soils has a portion due to friction and another due to viscosity.

Thomasi (2000), based on Martins (1992), proposed that the effective stress σ' is composed of two components:

[#]Corresponding author. E-mail address: raphaelfc1987@gmail.com
[1]Pesquisador Geotécnico Independente, Rio de Janeiro, RJ, Brasil.
[2]Universidade Federal do Rio de Janeiro, Departamento de Engenharia Civil, Rio de Janeiro, RJ, Brasil.
[3]Universidade Estadual do Rio de Janeiro, Departamento de Estruturas e Engenharia de Fundações, Rio de Janeiro, RJ, Brasil.

Submitted on April 10, 2024; Final Acceptance on October 7, 2024; Discussion open until May 31, 2025.
Editor: Renato P. Cunha

https://doi.org/10.28927/SR.2025.003124

one related to solid contacts, another related to viscous contacts:

$$\sigma = \sigma'_s\left(e\right) + \sigma'_\eta\left(e;\varepsilon\right) + u \tag{1}$$

where σ is the total stress, u is the pore pressure, σ'_s is the solid component, σ'_η is the viscous component. The solid component is a function only of the void ratio e, and its variation would be the true cause of deformations and distortions. The viscous component is a function of the strain rate $\dot{\varepsilon}$, and its variation would not cause deformations and distortions.

Other important studies of the influence of viscosity or the strain rate in soft soils are Taylor & Merchant (1940), Šuklje (1957), Hvorslev (1960), Gibson & Lo (1961), Barden (1965), Berry & Wilkinson (1969) and Bjerrum (1972), among many others. More recent studies are Zou et al. (2020), Schnaid et al. (2021) and Martins (2023).

Andrade (2014) developed a consolidation theory based on the model expressed by Equation 1. The relationship between the viscous component and the strain rate was assumed to be linear for simplification. Analytical solution introduced a new dimensionless parameter V, called Viscosity Factor. However, results were not able to show the secondary consolidation branch in the curves of average degree of consolidation, regardless the value of V. Andrade (2014) argued this was due to the linear relationship, as it should be non-linear. It is verified that Andrade (2014) theory is mathematically equivalent to Taylor (1942) theory.

Biz et al. (2022) proposed a modification to Andrade (2014) theory introducing a non-linear relationship. The viscous component was assumed to be a power function of the strain rate, based on Barden (1965), leading to a new expression for the Viscosity Factor V. Solution was obtained numerically. Results showed that the secondary consolidation branch is still absent for low values of V, but it is likely to appear for higher values. However, Biz et al. (2022) did not present the complete solution for higher V.

Alexandre & Thomasi (2023) proposed a non-linear consolidation theory made of a linear spring in series with a linear Kelvin-Voigt body, based on Gibson & Lo (1961) model. Total strain is divided into parts, related to primary and secondary compressions. Primary strain is a linear function of the effective stresses (as in classical theories), while secondary strain is a function of the strain rate, as the Kelvin-Voigt body represents structural viscous resistance to compression. Different equations for the Kelvin-Voigt body were proposed, and solutions were obtained numerically.

This paper aims develop theories of radial flow consolidation, for free strain and equal strain conditions, using the same model expressed by Equation 1. In order to investigate whether the manifestation of secondary consolidation is really dependent on the non-linearity of the viscous component in this model, linear and non-linear relationships will be addressed.

2. Fundamentals

2.1 Viscous component and secondary consolidation

Figure 1 shows Lima (1993) consolidation test, carried out in a triaxial cell on a clay sample from Sarapuí river, Rio de Janeiro. The drainage was closed at the end of primary consolidation, preventing volume changes and distortion. However, from the moment the drainage was closed, an increase in pore pressure was observed. According to the Principle of Effective Stress, if there is no change in volume or distortion, there should be no variation of the effective stress. And if the total stress is kept constant, there should be no increase in pore pressure either.

The interpretation of the phenomenon based on Equation 1 is as follows. The viscous component σ'_η can only exist if there is any strain rate $d\varepsilon / dt$. Closing the drainage makes $\dot{\varepsilon}$ go to zero, therefore causing a variation in σ'_η as it tends to zero as well. At the same time, the solid component σ'_s must remain constant, as there is no longer any variation in the void ratio e. Since the total stress σ is kept constant in the tests, the equality of Equation 1 can only prevail with the increase in pore pressure u. In this way, the effective stress would actually be varying, as there would be a transfer of its viscous component to the pore pressure. However, this would

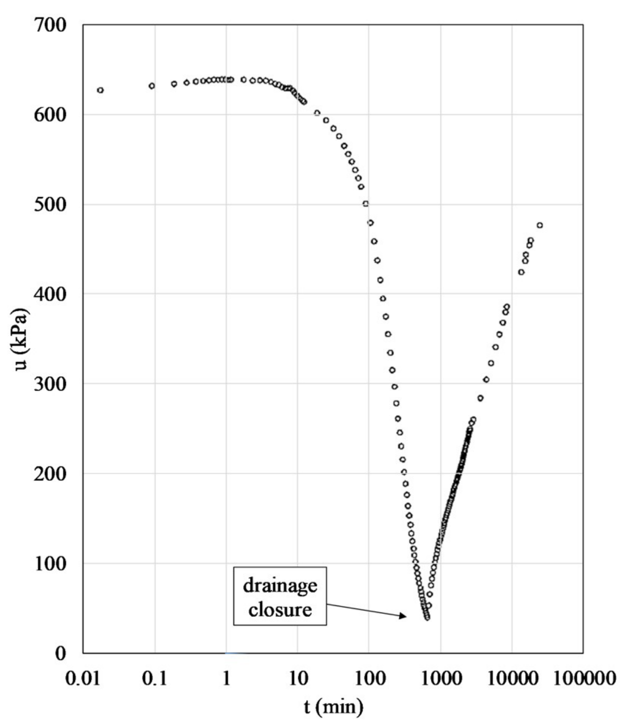

Figure 1. Increase in pore pressure after drainage closure at the end of primary consolidation (Lima, 1993).

not lead to any deformation or distortion on the specimen, since the variation of the viscous component does not cause these effects by definition.

Secondary consolidation can also be explained by this model. At the "end" of primary consolidation, the excess pore pressure is practically zero. Since the total stress is kept constant, the effective stress is assumed to be constant. This means the change in volume cannot be attributed to a change in effective stress as a whole. As suggested in Figure 1, the viscous component of the effective stress is still present in significant magnitude at the end of the primary. Thus, secondary consolidation would occur by the internal transfer of the viscous component σ'_η to the solid component σ'_s, so that the effective stress as a whole does not vary. The change in volume happens because the solid component is varying, and it is what actually causes deformations.

Therefore, primary consolidation occurs through a transfer of excess pore pressure to the solid component of the effective stress, while secondary consolidation occurs through a transfer of the viscous component of the effective stress to the solid component. Primary and secondary consolidation would not be two distinct phenomena, but the same phenomenon resulting from two effects that combine: hydrodynamic resistance to drainage and viscous resistance to deformation.

This understanding of the role of viscosity in soils is similar to but different from that of Taylor (1942). The viscous component is not an additional portion to the effective stress, but a part of it. And although it is a part of the effective stress, its variation does not cause deformations or distortions, as predicted by the Principle of Effective Stress. Thus, Equation 1 represents a slight change in the Principle of Effective Stress, as proposed by Martins (1992).

2.2 Components of the effective stress in the compression curve

There is an important consequence in the initial excess pore pressure. At time $t = 0^+$, when the load is instantaneously applied, the void ratio has not changed yet, which corresponds to a zero increase in the solid component of the effective stress. However, because the load is applied instantaneously, at this moment there is already a non-zero strain rate. This strain rate mobilizes the viscous component of the effective stress, mainly near the drainage boundaries, where it is higher.

This means that the initial increase in effective stress (solid component + viscous component) is actually greater than zero and, therefore, the initial excess pore pressure is smaller than the total stress increment applied. It is worth mentioning that Thomasi (2000) in fact observed an initial excess pore pressure lower than the total stress increase, when measuring pore pressure in consolidation tests carried out in a triaxial cell.

Figure 2 illustrates how the components of the vertical effective stress σ'_v and the pore pressure u are related in the compression curve. Segment ADGJ (Figure 2a) is the line of the end of consolidation (primary and secondary), corresponding to a strain rate $\dot{\varepsilon}_v$ equal to zero. It represents the relationship between the void ratio e and the solid component of the vertical effective stress σ'_{vs} – the component which is actually associated with change in volume. Each line parallel to the ADGJ is an isotache (a line of same strain rate). Curve BEHJ shows the excess pore pressure at any effective stress σ'_v, and AC is the total stress increase $\Delta\sigma_v$.

At $t = 0^+$, if consolidation begins at point A, segment AB is the value of the viscous component of the vertical effective stress $\sigma'_{v\eta}$ (non-zero, since there is already a strain rate from the beginning) and BC is the initial excess

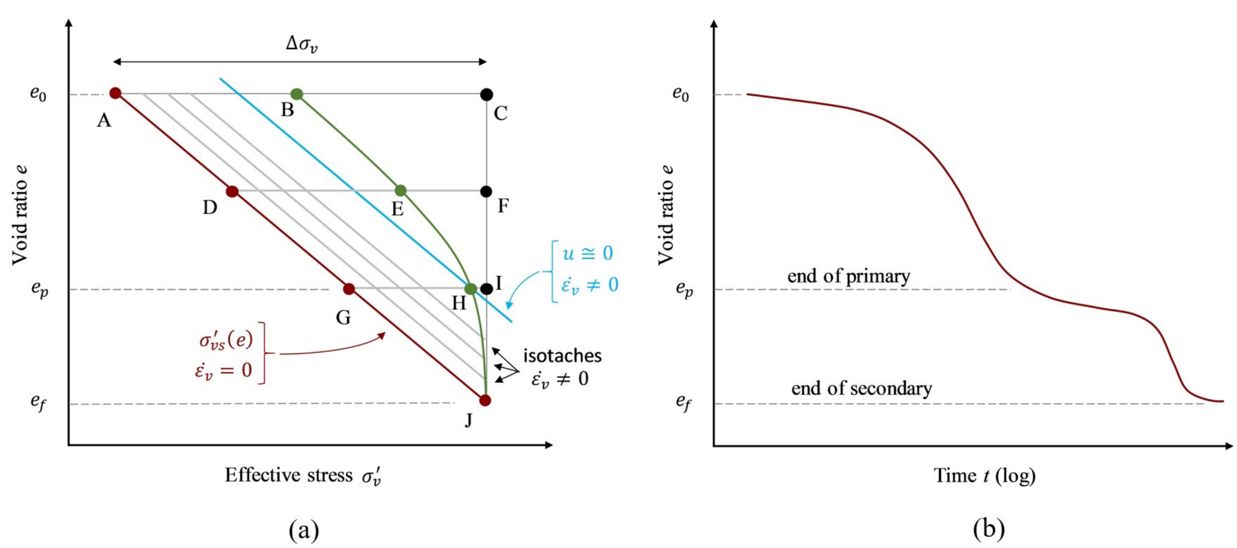

Figure 2. Primary and secondary compressions in the model. (a) Compression curve. (b) Consolidation curve.

pore pressure. The "movement" from point A to point B is a change in effective stress, but there is no deformation as there is no change in σ'_{vs} – void ratio is still the initial void ratio e_0. This is comparable to overconsolidation, as if segment AB could be interpreted as the recompression curve naturally emerging from the model, while point B would be the preconsolidation stress.

During consolidation, the magnitudes of the effective stress components and the excess pore pressure vary. At a given moment, the viscous component is represented by segment DE and the excess pore pressure by segment EF. After a certain time, the viscous component corresponds to segment GH, and segment HI is the excess pore pressure, so small that is negligible – this is the "end of the primary" for practical purposes, at void ratio e_p (Figure 2b). The path HJ, almost coincident with IJ, has been called in engineering practice "secondary compression". Consolidation ends at point J, when the void ratio is its final value e_f.

2.3 Andrade's theory

Andrade (2014) used this model to develop a new theory of one-dimensional consolidation. The relationship between the viscous component and the strain rate was assumed to be linear for simplification, which corresponds to a Newtonian behavior. The inclusion of viscosity led to the emergence of a new dimensionless parameter V, called Viscosity Factor:

$$V = \frac{\bar{\eta} k_z}{\gamma_w H_d^2} \tag{2}$$

where k_z is the coefficient of vertical permeability, γ_w is the unit weight of water, H_d is the maximum length of the drainage path, and $\bar{\eta}$ is the average viscosity coefficient, which is the coefficient of proportionality between the viscous component and the strain rate.

The Viscosity Factor acts to "delay" consolidation, both primary and secondary. The higher the value of V, the longer it takes for consolidation to develop. If $V = 0$ (that is, if $\bar{\eta} = 0$), the solution reduces to the classical theory (Terzaghi & Fröhlich, 1939), since there is no viscosity to slow down the process.

Figure 3 shows the attempt of fitting between the theory and experimental results carried out by Martins (1990), in a long-term consolidation test in a mixture of 90% kaolin and 10% bentonite. Andrade (2014) adopted $V = 0.008$ as the best fit. Although the model is capable of theoretically explaining secondary consolidation, the theory was clearly not capable of reproducing it as seen in the consolidation test.

Andrade (2014) argued that this result is due to the linearity of the relationship between the viscous component and the strain rate, for it should be non-linear. Figure 4 illustrates the reasoning. The viscosity coefficient is the tangent of the curve that relates the viscous component of the effective stress and the strain rate. For a non-linear relationship, $\eta = \eta_0$

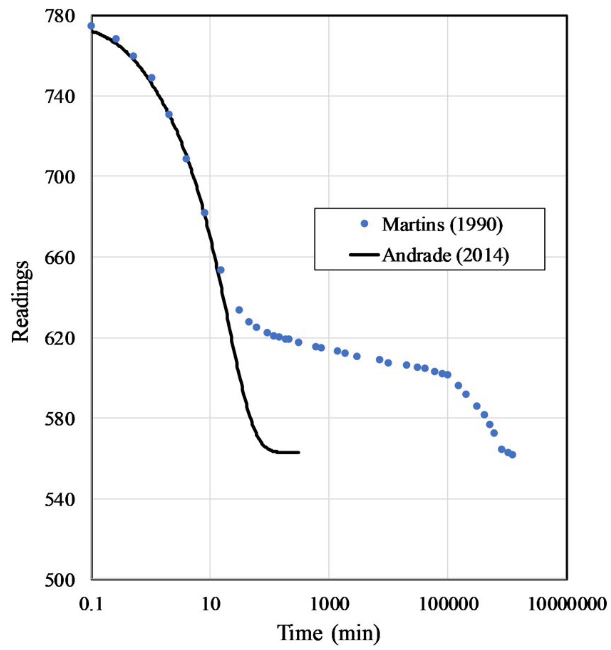

Figure 3. Comparison between experimental curve (Martins, 1990, from Andrade, 2014) and theoretical curve (Andrade, 2014) ($V = 0.008$).

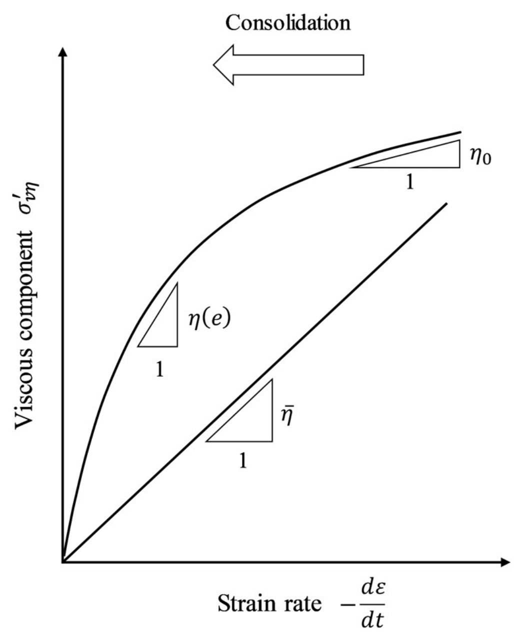

Figure 4. Viscous component versus strain rate.

at the beginning of consolidation is the smallest tangent. As consolidation proceeds, $\eta(e)$ grows until it reaches its maximum value at the end.

Andrade (2014) adopted a linear relationship using a constant value $\bar{\eta}$, searching for the best fit during primary consolidation – that is, $\bar{\eta}$ closer to η_0. Therefore, the viscous component was lower than expected for lower strain rates. This leads to an underestimation of the secondary consolidation, as it depends directly on the presence of the viscous component at the end of the primary.

Experimental evidence that the viscous component is non-Newtonian was presented by Alexandre (2000, 2006) and Santa Maria (2002). Santa Maria & Santa Maria (2018) suggested a hyperbola as a reasonable fit, as shown in Figure 5. It can be seen the tangent of the curve increases as the void ratio rate decreases.

In general, long-term consolidation tests exhibit the same behavior as Martins (1990) test (Figure 3). First, primary consolidation occurs, as predicted by the classical theory of consolidation (with no viscosity). Then, secondary consolidation becomes predominant, through an approximately constant slope in log scale – better known by the parameter C_α in the $e - \log t$ curve. Finally, after a long time, a change in slope marks the end of secondary consolidation, and consolidation as a whole. Other long-term tests for vertical flow consolidation were performed by Elrefai (1973), Salem & Krizek (1975), Félix (1980), Vieira (1988) and Carvalho (1997).

It is worth mentioning that Santa Maria & Santa Maria (2018) expanded the Newtonian theory proposed by Andrade (2014) by considering the compressibility of the water in the voids. An analytical solution was presented, and it matches Andrade's theory if the bulk modulus of elasticity of water tends to infinity (water is incompressible). In the present paper, however, the compressibility of water will not be addressed. Its influence is mainly at the very beginning of consolidation, while the objective of the present paper is to understand secondary consolidation as a function of the strain rate.

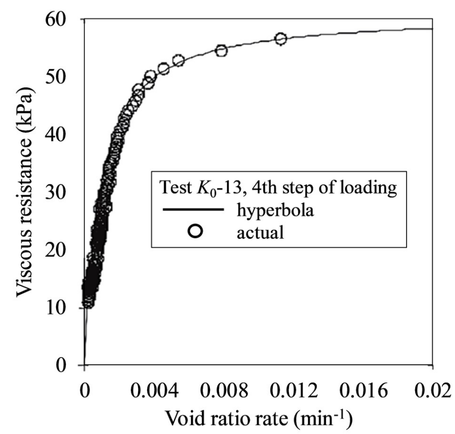

Figure 5. Viscous resistance versus void ratio rate – fitted hyperbola compared with one-dimensional consolidation data (Santa Maria, 2002, after Santa Maria & Santa Maria, 2018).

3. Radial flow consolidation theories

Since the model presented in this paper was used in consolidation theories only for vertical flow (Andrade, 2014; Santa Maria & Santa Maria, 2018), theories of consolidation for radial flow will be developed in this item. The differential equations can be solved using the same methods as Barron (1948) and Taylor & Merchant (1940). The complete solution is presented in Carneiro (2019).

Three theories will be developed and solved analytically:

- free strain condition – Newtonian behavior;
- equal strain condition – Newtonian behavior;
- equal strain condition – non-Newtonian behavior.

Some simplifying assumptions are the same as the classical theories of radial flow consolidation (Rendulic, 1935; Barron, 1948). They are:

- Soil is homogeneous;
- Soil is fully saturated;
- Grain and water compressibility is negligible compared to soil skeleton compressibility;
- Darcy's Law is valid;
- Water flows in a horizontal/radial plane (towards the drain well);
- Compression is one-dimensional;
- Some physical parameters remain constant over time.

Additional assumptions result from the components of the effective stress, absent from Barron (1948) theory:

- Effective vertical stress is made up of two components: a solid component and a viscous component;
- Volume change is due exclusively to variation in the solid component of the effective stress;
- Variation in the void ratio is proportional to variation in the solid component of the effective stress;
- The viscous component of effective stress is a function of strain rate;

From the simplifying assumptions in common with Barron (1948), the differential equation that serves as the basis for the three theories is:

$$\frac{k_r}{\gamma_w}\left(\frac{1}{r}\frac{\partial u}{\partial r}+\frac{\partial^2 u}{\partial r^2}\right)=\frac{1}{1+e}\frac{\partial e}{\partial t} \tag{3}$$

where k_r is the coefficient of radial permeability, γ_w is the unit weight of water, u is the excess pore pressure, e is the void ratio, r is the radius variable and t is the time variable.

3.1 Free strain condition – Newtonian behavior

In the free strain condition, volume changes are the result of uniform loading on the surface. From the model:

$$\sigma_v = \sigma'_{vs} + \sigma'_{v\eta} + u \tag{4}$$

Differentiating with respect to time:

$$\frac{d\sigma'_{vs}}{dt}+\frac{d\sigma'_{v\eta}}{dt}+\frac{du}{dt}=0 \tag{5}$$

Relating the void ratio with the solid component:

$$\frac{de}{dt}=\frac{de}{d\sigma'_{vs}}\frac{d\sigma'_{vs}}{dt} \tag{6}$$

The constant that defines the proportionality between the variation in the void ratio and the variation in the solid component will be represented by a_{vs}. It is worth noting that a_{vs} is analogous to a_v in classical theories of consolidation, but conceptually different as it refers to one of the effective stress components and not to the effective stress as a whole. From Equation 6:

$$\frac{de}{dt}=-a_{vs}\frac{d\sigma'_{vs}}{dt} \tag{7}$$

Now from Equation 5:

$$\frac{de}{dt}=a_{vs}\left(\frac{d\sigma'_{v\eta}}{dt}+\frac{du}{dt}\right) \tag{8}$$

As the viscous component in this theory presents Newtonian behavior, the same relation from Andrade (2014) will be adopted:

$$\sigma'_{v\eta}=-\frac{\overline{\eta}}{1+e}\frac{\partial e}{\partial t} \tag{9}$$

Differentiating $\sigma'_{v\eta}$ with respect to time and combining it with Equation 8:

$$\frac{de}{dt}=a_{vs}\left[\frac{du}{dt}-\left(\frac{\overline{\eta}}{1+e}\right)\frac{\partial^2 e}{\partial t^2}\right] \tag{10}$$

Combining Equations 3) and 10, it gives:

$$c_{rs}\left(\frac{1}{r}\frac{\partial u}{\partial r}+\frac{\partial^2 u}{\partial r^2}\right)+\left(\frac{k_r\overline{\eta}}{\gamma_w}\right)\frac{\partial}{\partial t}\left(\frac{1}{r}\frac{\partial u}{\partial r}+\frac{\partial^2 u}{\partial r^2}\right)-\frac{\partial u}{\partial t}=0 \tag{11}$$

where c_{rs} is the coefficient of radial consolidation given by:

$$c_{rs}=\frac{k_r\left(1+e\right)}{a_{vs}\gamma_w} \tag{12}$$

The boundary and initial conditions are:

- $u\left(r_w,t\right)=0$ for $t>0$;
- $\left.\frac{\partial u\left(r,t\right)}{\partial r}\right|_{r=r_e}=0$ for $t>0$;
- $u\left(r,0\right)=u_0\left(r\right)$ for $t=0$

where r_w is the radius of the well, r_e is the external radius (radius of influence), and $u_0\left(r\right)$ is the initial excess pore pressure as a function of the radius variable r.

It should be noticed that the two boundary conditions are identical to Barron (1948) classical theory of radial flow consolidation. However, the initial condition is different from Barron (1948) as viscosity causes the initial excess pore pressure to be less than the total vertical stress increase $\Delta\sigma_v$, as part of it becomes increase in the viscous component of the effective stress.

Solution in terms of normalized excess pore pressure $u\left(r,t\right)/\Delta\sigma_v$ is:

$$\frac{u\left(r,t\right)}{\text{Ä}\sigma_v}=\sum_{\alpha_1,\alpha_2,\alpha_3\ldots}^{\alpha_\infty}\frac{-2A_1\left(\alpha\right)A_0\left(\alpha n\frac{r}{r_e}\right)}{\alpha\left[n^2A_0{}^2\left(\alpha n\right)-A_1{}^2\left(\alpha\right)\right]} \left[\frac{1}{1+4\alpha^2n^2V_r}\right]\exp\left(-\frac{4\alpha^2n^2T_{rs}}{1+4\alpha^2n^2V_r}\right) \tag{13}$$

$$A_1\left(\alpha\right)=J_1\left(\alpha\right)Y_1\left(\alpha n\right)-Y_1\left(\alpha\right)J_1\left(\alpha n\right)$$

$$A_0\left(\alpha n\right)=J_0\left(\alpha n\right)Y_1\left(\alpha n\right)-Y_0\left(\alpha n\right)J_1\left(\alpha n\right)$$

$$A_0\left(\alpha n\frac{r}{r_e}\right)=J_0\left(\alpha n\frac{r}{r_e}\right)Y_1\left(\alpha n\right)-Y_0\left(\alpha n\frac{r}{r_e}\right)J_1\left(\alpha n\right)$$

where:

$_0$, J_1 – Bessel functions of the 1st kind of zero and first order, respectively;

Y_0, Y_1 – Bessel functions of the 2nd kind of zero and first order, respectively;

$\alpha_1, \alpha_2, \alpha_3, \ldots$ – roots satisfying $J_1\left(\alpha n\right)Y_0\left(\alpha\right)-Y_1\left(\alpha n\right)J_0\left(\alpha\right)=0$;

and n is the ratio:

$$n=\frac{r_e}{r_w}=\frac{d_e}{d_w} \tag{14}$$

where d_w is the diameter of the well and d_e is the external diameter.

The Radial Time Factor T_{rs} is given by:

$$T_{rs}=\frac{c_{rs}t}{d_e{}^2} \tag{15}$$

The Radial Viscosity Factor V_r is given by:

$$V_r=\frac{k_r\overline{\eta}}{\gamma_w d_e{}^2} \tag{16}$$

Finally, solution in terms of average degree of consolidation $\overline{U_r}$ is:

$$\overline{U_r} = 1 - \sum_{\alpha_1,\alpha_2,\alpha_3\ldots}^{\alpha_\infty} \frac{4A_1(\alpha)^2}{\alpha^2\left(n^2-1\right)\left[n^2A_0{}^2(\alpha n) - A_1{}^2(\alpha)\right]} \exp\left(-\frac{4\alpha^2n^2T_{rs}}{1+4\alpha^2n^2V_r}\right) \tag{17}$$

3.2 Equal strain condition – Newtonian behavior

In the equal strain condition, volume changes are uniform rather than the stress increases. This requires working with the averages of the stresses. From the model:

$$\overline{\sigma_v} = \overline{\sigma'_{vs}} + \overline{\sigma'_{v\eta}} + \overline{u} \tag{18}$$

Repeating the steps from Equations 3 to 10 for the averages of the stresses:

$$\frac{de}{dt} = a_{vs}\left[\frac{d\overline{u}}{dt} - \left(\frac{\overline{\eta}}{1+e}\right)\frac{\partial^2 e}{\partial t^2}\right] \tag{19}$$

Combining with Equation 3:

$$c_{rs}\left(\frac{1}{r}\frac{\partial u}{\partial r} + \frac{\partial^2 u}{\partial r^2}\right) + \left(\frac{k_r\overline{\eta}}{\gamma_w}\right)\frac{\partial}{\partial t}\left(\frac{1}{r}\frac{\partial u}{\partial r} + \frac{\partial^2 u}{\partial r^2}\right) - \frac{d\overline{u}}{dt} = 0 \tag{20}$$

With the following boundary and initial conditions:

- $u(r_w,t) = 0$ for $t > 0$;
- $\left.\frac{\partial u(r,t)}{\partial r}\right|_{r=r_e} = 0$ for $t > 0$;
- $\overline{u}(0) = \overline{u_0}$ for $t = 0$

where $\overline{u_0}$ is the initial average excess pore pressure, again less than the total vertical stress increase $\Delta\sigma_v$.

Solution in terms of normalized excess pore pressure $u(r,t)/\Delta\sigma_v$ is:

$$\frac{u(r,t)}{\text{Ä}\sigma_v} = \frac{\frac{1}{8}}{\frac{f(n)}{8}+V_r}\left[\ln\left(n\frac{r}{r_e}\right) - \frac{\left(\frac{r}{r_e}\right)^2 - \frac{1}{n^2}}{2}\right] \exp\left(\frac{-T_{rs}}{\frac{f(n)}{8}+V_r}\right) \tag{21}$$

where T_{rs} and V_r are expressed by Equations 15 and 16, and

$$f(n) = \frac{n^2}{n^2-1}\ln n - \frac{3n^2-1}{4n^2} \cong \ln n - \frac{3}{4} \tag{22}$$

And in terms of average degree of consolidation $\overline{U_r}$ is:

$$\overline{U_r} = 1 - \exp\left[\frac{-8T_{rs}}{f(n)+8V_r}\right] \tag{23}$$

3.3 Equal strain condition – non-Newtonian behavior

The average viscous component of the effective stress $\overline{\sigma'_{v\eta}}$ is defined as:

$$\overline{\sigma'_{v\eta}} = -\frac{\eta(e)}{1+e}\frac{\partial e}{\partial t} \tag{24}$$

In this development a function $\eta(e)$ that increases with time will be used, instead of an average value $\overline{\eta}$. The aim of this theory is to obtain an analytical solution to the problem, thus $\sigma'_{v\eta}$ as a function of the strain rate will not be a hyperbola, as suggested by Santa Maria & Santa Maria (2018). Let $\eta(e)$ be expressed by:

$$\eta(e) = \eta_f - \left(\eta_f - \eta_0\right)a_u\frac{\partial\overline{u}}{\partial e} \tag{25}$$

where η_0 and η_f are the initial and final values of the viscosity coefficient, respectively, and a_u is the value, at time $t = 0$, of the following derivative:

$$a_u = \left.\frac{\partial e}{\partial\overline{u}}\right|_{t=0} \rightarrow \frac{1}{a_u} = \left.\frac{\partial\overline{u}}{\partial e}\right|_{t=0} \tag{26}$$

The value of $\partial\overline{u}/\partial e$ is maximum for $t = 0$, as most of the initial deformation is caused by the transfer of excess pore pressure to the solid component. It can be noticed that, at $t = 0$, Equation 25 gives $\eta(e) = \eta_0$. Near the end of the consolidation, $\partial\overline{u}/\partial e$ tends to 0, since all the excess pore pressure has dissipated. Thus, $\eta(e)$ tends to its final value $_f$. Therefore, $\eta(e)$ is smaller at the beginning and grows as the consolidation takes place.

It should be made clear that the Equation 25 is not a theoretical relationship, nor even verified experimentally. It is a mathematical expression to make the viscous component non-linear and, at the same time, to allow an analytical solution for the differential equation. However, the idea that the value of $\eta(e)$ increases with time is in fact based on experimental results.

Let λ be:

$$\frac{\eta_f - \eta_0}{\eta_f} = \lambda \tag{27}$$

which varies between 0 and 1. If $\lambda = 0$, the final viscosity coefficient η_f is equal to the initial one η_0. This is the case of constant viscosity coefficient.

Rewriting Equation 25:

$$\eta(e) = \eta_f - \lambda a_u \eta_f \frac{\partial \overline{u}}{\partial e} \tag{28}$$

Substituting Equation 28 into 24:

$$\overline{\sigma'_{v\eta}} = -\left(\eta_f - \lambda a_u \eta_f \frac{\partial \overline{u}}{\partial e}\right)\frac{1}{1+e}\frac{\partial e}{\partial t} \tag{29}$$

Rewriting it:

$$\overline{\sigma'_{v\eta}} = -\frac{\eta_f}{1+e}\frac{\partial e}{\partial t} + \lambda a_u \frac{\eta_f}{1+e}\frac{d\overline{u}}{dt} \tag{30}$$

Repeating the same process as in the previous items, it gives:

$$\begin{aligned} &c_{rs}\left(\frac{1}{r}\frac{\partial u}{\partial r} + \frac{\partial^2 u}{\partial r^2}\right) + \left(\frac{k_r \eta_f}{\gamma_w}\right)\frac{\partial}{\partial t}\left(\frac{1}{r}\frac{\partial u}{\partial r} + \frac{\partial^2 u}{\partial r^2}\right) - \\ &\lambda a_u \left(\frac{\eta_f}{1+e}\right)\frac{d^2\overline{u}}{dt^2} - \frac{d\overline{u}}{dt} = 0 \end{aligned} \tag{31}$$

From Figure 2, it is observed that the compression curve BEHJ at $t = 0$ has approximately the same tangent as the line of the end of consolidation ADGJ. In physical terms, this means that the initial volume change is entirely due to the transfer of the excess pore pressure to the effective stress at the beginning of consolidation. This is consistent, since consolidation tests provide primary consolidation curves very close to those predicted by classical theories, which are purely hydrodynamic.

Thus, boundary and initial conditions are:

- $u(r_w, t) = 0$ for $t > 0$;
- $\left.\dfrac{\partial u(r,t)}{\partial r}\right|_{r=r_e} = 0$ for $t > 0$;
- $\overline{u}(0) = \overline{u_0}$ for $t = 0$;
- $\dfrac{d\overline{u}}{dt} = c_{rs}\left(\dfrac{1}{r}\dfrac{\partial u}{\partial r} + \dfrac{\partial^2 u}{\partial r^2}\right)$ for $t = 0$.

The last condition is equal to the differential equation from Barron (1948). Thus, it is mathematically expressed that the very beginning of consolidation behaves as in classical theory, as interpreted from Figure 2 and observed in consolidation tests. Consequently, the viscous component $\overline{\sigma'_{v\eta}}$ is constant at the very beginning of consolidation ($d\sigma'_{v\eta}/dt = 0$), and $a_u = a_{vs}$.

Solution in terms of normalized excess pore pressure $\dfrac{u(r,t)}{\Delta\sigma_v}$ is:

$$\frac{u(r,t)}{\text{Ä}\sigma_v} = \frac{\frac{1}{8}}{\frac{f(n)}{8} + V_{rf}(1-\lambda)} \left\{ \frac{ X_1\left(1 + \frac{f(n)}{8}X_1\lambda\right)\exp(X_2 T_{rs}) - X_2\left(1 + \frac{f(n)}{8}X_2\lambda\right)\exp(X_1 T_{rs}) }{ X_1\left(1 + \frac{f(n)}{8}X_1\lambda\right) - X_2\left(1 + \frac{f(n)}{8}X_2\lambda\right) } \right\} \left[\ln\left(n\frac{r}{r_e}\right) - \frac{\left(\frac{r}{r_e}\right)^2 - \frac{1}{n^2}}{2} \right] \tag{32}$$

$$X_1 = \frac{-\left[\frac{f(n)}{8} + V_{rf}\right] + \sqrt{\left[\frac{f(n)}{8} + V_{rf}\right]^2 - 4\lambda\frac{f(n)}{8}V_{rf}}}{2\lambda\frac{f(n)}{8}V_{rf}}$$

$$X_2 = \frac{-\left[\frac{f(n)}{8} + V_{rf}\right] - \sqrt{\left[\frac{f(n)}{8} + V_{rf}\right]^2 - 4\lambda\frac{f(n)}{8}V_{rf}}}{2\lambda\frac{f(n)}{8}V_{rf}}$$

where T_{rs} is expressed by Equation 15, and the final Radial Viscosity Factor V_{rf} is:

$$V_{rf} = \frac{k_r \eta_f}{\gamma_w d_e^{\,2}} \tag{33}$$

And solution in terms of average degree of consolidation $\overline{U_r}$ is:

$$\overline{U_r} = 1 - \frac{V_{rf}}{\frac{f(n)}{8} + V_{rf}(1-\lambda)} \left\{ \frac{ \frac{X_1}{X_2}\left[1 + \frac{f(n)}{8}\lambda X_1\right]\exp(X_2 T_{rs}) - \frac{X_2}{X_1}\left[1 + \frac{f(n)}{8}\lambda X_2\right]\exp(X_1 T_{rs}) }{ (X_1 - X_2)\frac{f(n)}{8} } \right\} \tag{34}$$

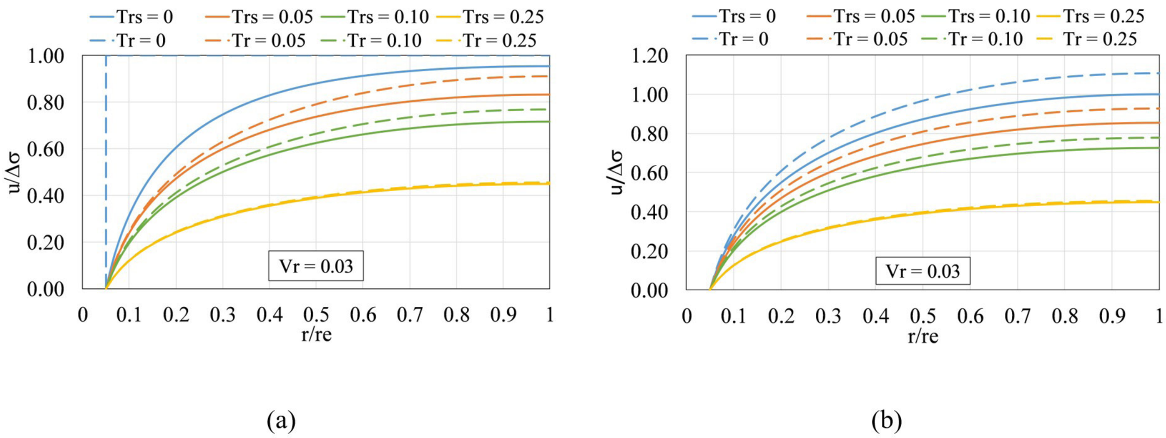

Figure 6. Isochrones $u(r,t)/\Delta\sigma_v$ versus r/r_e for Newtonian viscous component, with $n = 20$ and $V_r = 0.03$ (solid line), compared to Barron (1948) (dashed line). (a) Free strain; (b) Equal strain.

From Equation 27, it can be noticed that the term $V_{rf}(1-\lambda)$ in Equations 32 and 34 expresses the initial Radial Viscosity Factor V_{r0}:

$$V_{r0} = V_{rf}(1-\lambda) = \frac{k_r \eta_0}{\gamma_w d_e^{\,2}} \tag{35}$$

4. Results and discussion

The solutions obtained in the previous item depend on the Radial Viscosity Factor, V_r. This new dimensionless parameter is directly proportional to η, be it constant or variable. Being constant, the expression (Equation 16) is equivalent to that obtained by Andrade (2014) for vertical flow consolidation (Equation 2). Being variable, V_r can be expressed either by its final value, V_{rf}, or by its initial value, V_{r0}.

The Radial Time Factor, T_{rs}, is analogous to the Radial Time Factor from Barron (1948) theory. The difference between the two parameters is only conceptual, due to the assumption that deformations are caused by change in one component of the effective stress, and not the whole effective stress. Thus, T_{rs} is a function of $a_{vs} = -de/d\sigma'_{vs}$ instead of $a_v = -de/d\sigma'_v$. It should be noticed that Barron (1948) theory is a particular case of the present theory for zero viscosity, in which a_{vs} becomes identical to a_v.

4.1 Newtonian behavior

Figure 6 shows the isochrones relating the normalized excess pore pressure $u(r,t)/\Delta\sigma_v$ and the dimensionless radius r/r_e for Newtonian viscous component ($\eta(e) = \overline{\eta}$), for both free strain (Figure 6a) and equal strain (Figure 6b) conditions. Curves were plotted for $V_r = 0.03$ and $n = 20$. For comparison, Barron (1948) curves are also plotted, in dashes, relating T_r and T_{rs}. As mentioned, Barron (1948) solution is a particular case of the present theories when $\overline{\eta} = 0$ (no viscosity).

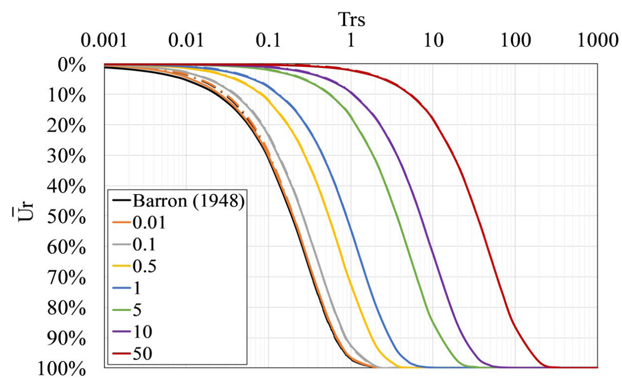

Figure 7. Comparison between average degree of consolidation curves for free strain (solid line) and equal strain (dashed line) conditions, for Newtonian viscous component and $n = 20$.

In general, the presence of viscosity "delays" the consolidation in the new theories when compared with the classical solution (Barron, 1948). The greater the value of V_r, the greater the delay. However, the behavior of the curves is quite similar for $V_r = 0.03$, as shown in Figure 6. It is worth mentioning that this value is almost 40 times greater than the best fit obtained by Andrade (2014) for the curves of the experimental tests performed by Martins (1990) (Figure 3).

In the free strain condition (Figure 6a), the presence of viscosity makes the initial pore pressure excess not equal to the total stress increase along the radius of influence of the well. This effect is more noticeable near the drainage boundary (at $r/r_e = 0.05$), because the strain rate is higher in this region.

Figure 7 compares the average degree of consolidation curves for free strain (solid line) and equal strain (dashed line) conditions, for Newtonian viscous component and $n = 20$. The curves from the classical theory (Barron, 1948), which correspond to $V_r = 0$, are also plotted. It can be noticed that, for $V_r < 0.1$, the curves are practically coincident with the classical theory. The higher the V_r values, the more they move away from Barron (1948), delaying consolidation. Furthermore, the difference between free strain and equal strain conditions is negligible.

More importantly, Figure 7 shows that the adoption of Newtonian behavior for the viscous component of the effective stress is not able to reproduce secondary consolidation. Viscosity delays consolidation not only after the excess pore pressure is practically zero, but the entire consolidation as a whole. This result is consistent with that obtained by Andrade (2014) for a vertical flow.

4.2 Non-Newtonian behavior

Figure 8 shows the isochrones relating the normalized excess pore pressure $u(r,t)/\Delta\sigma_v$ and the dimensionless radius r/r_e for the two theories of equal strain conditions, for $n = 20$. Curves for Non-Newtonian viscous component (solid lines) were plotted for $V_{r0} = 0.03$ and $V_{rf} = 10000$. Curves for Newtonian viscous component (dashed lines) were plotted for $V_r = 0.03$. It can be noticed that the two theories are almost coincident with respect to excess pore pressure. The value of the final Radial Viscosity Factor, even though it is so much higher than the initial one, makes a negligible difference in the results. Notice that the theory for the non-Newtonian viscous component converges to the Newtonian one by making $V_{rf} = V_{r0}$, as if the parameter η did not vary during consolidation.

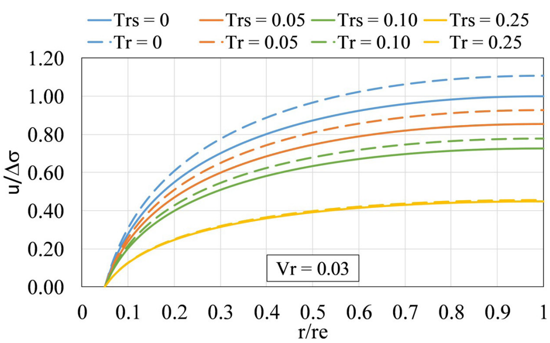

Figure 8. Comparison between average degree of consolidation curves for equal strain conditions, for non-Newtonian (solid line) and Newtonian (dashed line) viscous component, and $n = 20$.

Figure 9 shows the average degree of consolidation curves for equal strain condition for non-Newtonian viscous component, with $n = 20$, $V_{r0} = 0.1$ and different values of V_{rf}. It can be noticed that this theory is capable of presenting secondary consolidation. As all curves have the same V_{r0}, they all have the same ratio between primary settlement and total settlement, R. Thus, they form an asymptote at $\overline{U}_r = R$.

It was not possible to find radial flow consolidation tests in the literature long enough to observe the end of secondary consolidation. However, the behavior is expected to be comparable to those of vertical flow (Figure 3). Thus, the non-Newtonian theory (Figure 9) provided much more accurate results than the Newtonian theories (Figure 7).

Figure 10 shows the average degree of consolidation curves for the same case as Figure 9, but now with $V_{rf} = 10000$ for all curves and different values of V_{r0} for each one. As a result, each curve has a different ratio R, but they all tend to "end" consolidation at the same time as all of them have the same V_{rf} (which is an approximation since the end of consolidation is

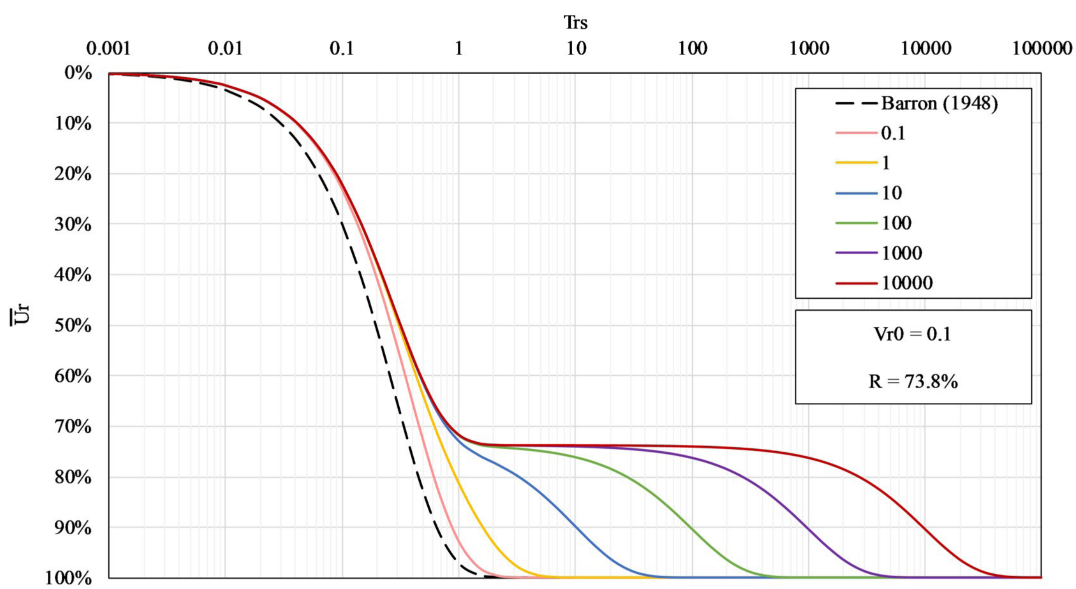

Figure 9. Average degree of consolidation curves for equal strain condition for non-Newtonian viscous component, with $n = 20$, $V_{r0} = 0.1$ and different values of V_{rf}.

theoretically at infinity). Barron (1948) theory corresponds to $R = 100\%$, since there is no secondary consolidation. The higher the V_{r0}, the smaller the portion of primary settlement in relation to the total settlement.

The interpretation of the previous figures (Figure 8, Figure 9 and Figure 10) makes it clear that V_{r0} is directly related to primary consolidation, while V_{rf} is related to secondary consolidation. The greater the value of V_{r0}, the smaller the portion of primary settlement in relation to the total. The greater the value of V_{rf}, the longer it takes for secondary consolidation to "end". Thus, as expected, V_{rf} has very little influence on the distribution of excess pore pressure, which is mainly dependent on V_{r0}.

From Figure 9, a curve with V_{rf} tending to infinity would be asymptotic at $\overline{U_r} = R$. By making $V_{rf} \to \infty$ in Equation 34, it gives:

$$\lim_{V_{rf} \to \infty} \overline{U_r} = R - \frac{\frac{f(n)}{8}}{\frac{f(n)}{8} + V_{r0}} \exp\left(-\frac{8T_{rs}}{f(n)}\right) \tag{36}$$

If $T_{rs} = 0$, then $\overline{U_r} = 0$. Therefore:

$$R = \frac{\frac{f(n)}{8}}{\frac{f(n)}{8} + V_{r0}} \to V_{r0} = \frac{f(n)}{8}\left(\frac{1-R}{R}\right) \tag{37}$$

Substituting into Equation 36:

$$\lim_{V_{rf} \to \infty} \overline{U_r} = R\left[1 - \exp\left(-\frac{8T_{rs}}{f(n)}\right)\right] \tag{38}$$

It can be noticed that Equation 38 is almost identical to the average degree of consolidation from Barron (1948) theory, differing only by the ratio R that multiplies the whole equation. This means that the primary consolidation from the present theory is in fact identical to that from Barron (1948).

The average initial excess pore pressure $\frac{\overline{u_0}}{\Delta\sigma_v}$ on the surface of the cylinder of influence of the well is defined as:

$$\frac{\overline{u_0}}{\Delta\sigma_v} = \frac{\overline{u}(0)}{\Delta\sigma_v} = \frac{\int_{r_w}^{r_e} \frac{u(r,0)}{\Delta\sigma_v} 2\pi r dr}{\pi\left(r_e^2 - r_w^2\right)} \tag{39}$$

From Equation 32, the following relation is obtained:

$$\frac{\overline{u_0}}{\Delta\sigma_v} = \frac{\frac{f(n)}{8}}{\frac{f(n)}{8} + V_{r0}} = R \tag{40}$$

Thus, in this theory the average initial excess pore pressure in relation to the total stress increase is equal to the magnitude of the primary settlement in relation to the total settlement. Although the initial excess pore pressure is expected to be lower than the total stress increase due to the effect of viscosity, this result is likely due to the linear

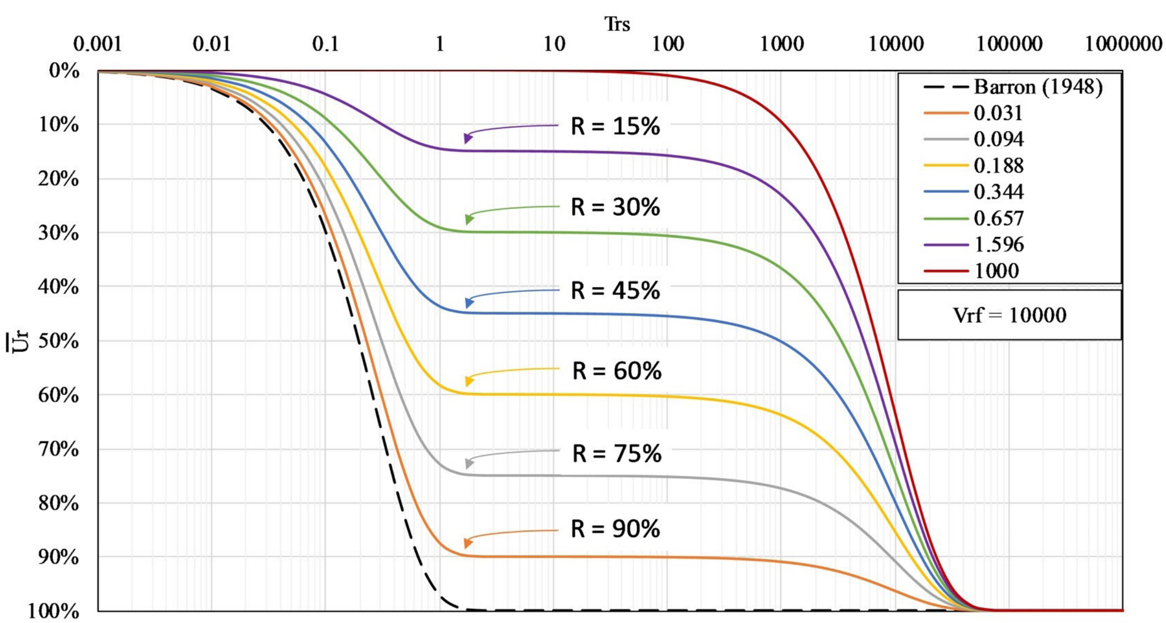

Figure 10. Average degree of consolidation curves for equal strain condition for non-Newtonian viscous component, with $n = 20$, $V_{rf} = 10000$ and different values of V_{r0}.

relationship between the variation in void ratio and the variation in the solid component of the effective stress, represented by the parameter a_{vs}.

Lastly, it can be noted that, although the theory is able to reproduce secondary consolidation, it is not able to show its characteristic slope C_α in log scale. The average degree of consolidation curves in Figure 9 are horizontally asymptotic, that is, with zero slope. It was seen that V_{r0} (and by extension η_0) determines the magnitude of primary settlement in relation to the total settlement, while V_{rf} (and by extension η_f) determines the time required for the "end" of secondary consolidation to occur. It is likely that the shape of the $\sigma'_{v\eta} - \partial e / \partial t$ curve is responsible for the slope C_α that connects the "end" of primary to the" end" of secondary, since it is essentially the transition from η_0 to η_f.

5. Conclusion

Three theories of radial flow consolidation were developed and solved analytically, with different behaviors for the viscous component $\sigma'_{v\eta}$ of the effective stress as a function of the strain rate $\partial \varepsilon / \partial t$. Results show that the Newtonian behavior is not able to reproduce secondary consolidation as seen in oedometer tests, since viscosity delays the entire consolidation as a whole.

On the other hand, the non-Newtonian behavior was able to properly display both primary and secondary consolidations, delaying only secondary compression. Consolidation curves for the non-Newtonian theory exhibit a clear distinction between primary and secondary compressions. Furthermore, the primary consolidation portion of the curve coincides with Barron (1948) classical theory.

Despite showing the distinction between primary and secondary consolidation, the non-Newtonian theory was not able to show the secondary compression index C_α. Instead, the average degree of consolidation curves are horizontally asymptotic during the transition from primary to secondary consolidation. Thus, results are highly dependent on the $\sigma'_{v\eta} - \partial \varepsilon / \partial t$ relationship adopted in the model.

The theories gave rise to a new dimensionless parameter called Radial Viscosity Factor, V_r. In theories for Newtonian behavior, V_r is a constant. In the non-Newtonian theory, the initial value V_{r0} determines the magnitude of the primary settlement in relation to the total settlement, while the final value V_{rf} determines the time required for the end of secondary consolidation.

Acknowledgements

The authors thank the Brazilian research agency CAPES for their support.

Declaration of interest

The authors have no conflicts of interest to declare. All co-authors have observed and affirmed the contents of the paper and there is no financial interest to report.

Authors' contributions

Raphael Felipe Carneiro: conceptualization, formal analysis, methodology, validation, writing – original draft. Ian Schumann Marques Martins: formal analysis, validation. Denise Maria Soares Gerscovich: visualization, validation, writing – review & editing.

Data availability

All data produced or examined in the course of the current study are included in this article.

Declaration of use of generative artificial intelligence

This work was prepared without the assistance of any generative artificial intelligence (GenAI) tools or services. All aspects of the manuscript were developed solely by the authors, who take full responsibility for the content of this publication.

List of symbols and abbreviations

a_u	$\partial e / \partial u$ at $t = 0$
a_v	Coefficient of compressibility
a_{vs}	Coefficient of compressibility in relation to σ'_{vs}
c_{rs}	Coefficient of radial consolidation in relation to σ'_{vs}
d_e	Diameter of influence of the well
d_w	Diameter of the well
e	Void ratio
e_0	Initial void ratio
e_p	Void ratio at the end of primary consolidation
e_f	Void ratio at the end of secondary consolidation
k_r	Coefficient of radial permeability
k_z	Coefficient of vertical permeability
n	Ratio of d_e and d_w
r	Radius
r_e	Radius of influence of the well
r_w	Radius of the well
t	Time
u	Pore pressure
u_0	Initial pore pressure
$\overline{u}$	Average pore pressure
$\underline{u_0}$	Average initial pore pressure
C_α	Coefficient of secondary consolidation
H_d	Maximum length of the drainage path in vertical flow consolidation

T_{rs}	Radial Time Factor in relation to σ'_{vs}
$\overline{U_r}$	Average degree of radial consolidation
V	Viscosity Factor
V_r	Radial Viscosity Factor
V_{r0}	Initial Radial Viscosity Factor
V_{rf}	Final Radial Viscosity Factor
γ_w	Unit weight of water
$\Delta\sigma_v$	Total stress increase
ε	Strain
$\dot{\varepsilon}$	Strain rate
$\overline{\eta}$	Average viscosity coefficient
η_0	Initial viscosity coefficient
η	Viscosity coefficient
η_f	Final viscosity coefficient
λ	Viscosity parameter relating $_0$ and η_f
σ	Total stress
σ'	Effective stress
σ'_s	Solid component of the effective stress
σ_η	Viscous component of the effective stress
σ_v	Vertical total stress
σ'_v	Vertical effective stress
σ'_{vs}	Solid component of the vertical effective stress
$\sigma'_{v\eta}$	Viscous component of the vertical effective stress
$\overline{\sigma_v}$	Average vertical total stress
$\overline{\sigma_{vs}}$	Average solid component of the vertical effective stress
$\overline{\sigma_{v\eta}}$	Average viscous component of the vertical effective stress

References

Alexandre, G.F. (2000). *A fluência não-drenada segundo o Modelo de Martins (1992)* [Master's dissertation]. COPPE/UFRJ (in Portuguese).

Alexandre, G.F. (2006). *Contribuição ao entendimento da fluência não-drenada* [Doctoral thesis]. COPPE/UFRJ (in Portuguese).

Alexandre, G. F., & Thomasi, L. (2023). A non-linear consolidation theory for soils exhibiting secondary compression. *HAL Open Science*, hal-03839465v2. In press.

Andrade, M.E.S. (2014). *Uma teoria de adensamento unidimensional considerando a resistência viscosa à compressão* [Doctoral thesis]. COPPE/UFRJ (in Portuguese).

Atkinson, J.H., & Bransby, P.L. (1978). *The mechanics of soils: an introduction to critical state soil mechanics* (375 p.). London: McGraw-Hill.

Barden, L. (1965). Consolidation of clay with non-linear viscosity. *Geotechnique*, 15(4), 345-362. http://doi.org/10.1680/geot.1965.15.4.345.

Barron, R.A. (1948). Consolidation of fine-grained soils by drains wells. *Transactions of the American Society of Civil Engineers*, 113(1), 718-742. http://doi.org/10.1061/TACEAT.0006098.

Berry, P.L., & Wilkinson, W.B. (1969). The radial consolidation of clay soils. *Geotechnique*, 19(2), 253-284. http://doi.org/10.1680/geot.1969.19.2.253.

Biz, J.C., Andrade, M.E.S., & Silva, E.C.S. (2022). A mathematical approach for predicting the consolidation of saturated clays. *Ciência e Natura*, 43, e2. http://doi.org/10.5902/2179460X66836.

Bjerrum, L. (1972). Embankments on soft ground. In *Proceedings of the ASCE Specialty Conference on Performance of Earth and Earth Supported Structures*, West Laffayette (Vol. 2, pp. 1-54). Purdue University.

Carneiro, R.F. (2019). *Adensamento unidimensional com fluxo radial considerando a viscosidade dos solos e a compressão secundária* [Doctoral thesis]. Rio de Janeiro State University (in Portuguese).

Carvalho, S.R.L. (1997). *Uma teoria de adensamento com compressão secundária* [Doctoral thesis]. COPPE/UFRJ (in Portuguese).

Elrefai, A. (1973). *Time dependent deformation of cohesive soils* [Doctoral thesis]. The Ohio State University.

Félix, B. (1980). *Le fluage et la consolidation unidimensionnelle des sols argileux* (Rapport de Recherché LPC, No. 94). Paris: Laboratoire Central des Ponts et Chaussées (in French).

Gibson, R. E., & Lo, K. Y. (1961). *A theory of consolidation for soils exhibiting secondary compression* (41 p.). Oslo: Norwegian Geotechnical Institute (also Acta Polytechnica Scandinavica, 296/191, Ci 10).

Hvorslev, M.J. (1960). Physical components of the shear strength of saturated clays. In *Proceedings of the Research Conference on Shear Strength of Cohesive Soils* (pp. 169-273). ASCE.

Leroueil, S., Kabbaj, M., Tavenas, F., & Bouchard, R. (1985). Stress-strain-strain rate relation for the compressibility of sensitive natural clays. *Geotechnique*, 35(2), 159-180. http://doi.org/10.1680/geot.1985.35.2.159.

Lima, G.P. (1993). *Estudo de uma teoria não-linear para o adensamento unidimensional* [Master's dissertation]. COPPE/UFRJ (in Portuguese).

Martins, I.S.M. (1990). [*Unpublished research report*]. (in Portuguese).

Martins, I.S.M. (1992). *Fundamentos de um modelo de comportamento de solos argilosos saturados* [Doctoral thesis]. COPPE/UFRJ (in Portuguese).

Martins, I.S.M. (2023). The 8th Victor de Mello lecture: role played by viscosity on the undrained behaviour of normally consolidated clays. *Soils and Rocks*, 46(3), e2023006123. http://doi.org/10.28927/SR.2023.006123.

Rendulic, L. (1935). Der Hydrodynamische Spannungsaugleich in Zentral Entwässerten Tonzylindern. *Wasserwirtschaft und Technik*, 2, 250-273.

Santa Maria, F.C.M. (2002). *Estudo reológico-experimental do coeficiente de empuxo no repouso, K0* [Doctoral thesis]. COPPE/UFRJ (in Portuguese).

Santa Maria, P.E.L., & Santa Maria, F.C.M. (2018). One-dimensional consolidation considering viscous soil behaviour and water compressibility – viscoconsolidation. *Soils and Rocks*, 41(1), 33-48. http://doi.org/10.28927/SR.411033.

Salem, A.M., & Krizek, R.J. (1975). Secondary compression of maintenance dredgings. In *Proceedings of the 5th Panamerican Conference on Soil Mechanics and Foundation Engineering* (Vol. 3, pp. 105-113), Buenos Aires.

Schnaid, F., Martins, I.S.M., Delgado, B.G., & Odebrecht, E. (2021). Strain rates effects in the prediction of geotechnical parameters. *Geotecnia*, 152, 405-434. http://doi.org/10.14195/2184-8394_152_12.

Šuklje, L. (1957). The analysis of the consolidation process by the isotaches method. In *Proceedings of the 4th International Conference on Soil Mechanics and Foundation Engineering* (Vol. 1, pp. 200-206), London.

Taylor, D.W., & Merchant, W. (1940). A theory of clay consolidation accounting for secondary compression. *Journal of Mathematics and Physics*, 19(1-4), 167-185. http://doi.org/10.1002/sapm1940191167.

Taylor, D.W. (1942). *Research on consolidation of clays* (MIT Series, No. 82, 147 p.). Cambridge: Department of Civil and Sanitary Engineering, Massachusetts Institute of Technology.

Terzaghi, K. (1941). Undisturbed clay samples and undisturbed clays. *Journal of Boston Society of Civil Engineers*, *XXVIII*(3). [Republished in *Contributions to Soil Mechanics* 1941-1959, Boston Society of Civil Engineers, Boston, pp. 45-65].

Terzaghi, K. F., & Fröhlich, O.K. (1939). *Théorie du tassement des couches argileuses: introduction à la mécanique analytique des argiles.* Paris (in French).

Thomasi, L. (2000). *Sobre a existência de uma parcela viscosa na tensão normal efetiva* [Master's dissertation]. COPPE/UFRJ (in Portuguese).

Vieira, L.O.M. (1988). *Contribuição ao estudo do adensamento secundário* [Master's dissertation]. COPPE/UFRJ (in Portuguese).

Zou, S.F., Xie, X.Y., Li, J.Z., Wang, Z.J., & Lehane, B.M. (2020). One dimensional formulae for time-dependent compression characteristics of over-consolidated clays. *Computers and Geotechnics*, 119, 103364. http://doi.org/10.1016/j.compgeo.2019.103364.